Noncanonical microglial IL-1β maturation in chronic kidney disease

Silke Zimmermann[1], Akash Mathew[1], Olga Bondareva[2], Ahmed Elwakiel[1], Shihai Jiang[1], Rajiv Rana[1], Ingo Bechmann[3], Jürgen Goldschmidt[4], Nora Klöting[2], Bilal N. Sheikh[2], Berend Isermann[1]

1 Institute of Laboratory Medicine, Clinical Chemistry, and Molecular Diagnostics, University Hospital, Leipzig, Germany

2 Helmholtz Institute for Metabolic, Obesity and Vascular Research (HI-MAG) of the Helmholtz Center Munich, Leipzig, Germany

3 Institute of Anatomy, Leipzig University, Leipzig, Germany

4 Leibniz Institute for Neurobiology, Magdeburg, Germany

Correspondence to:

Berend Isermann or Silke Zimmermann;

E-mail: berend.isermann@medizin.uni-leipzig.de or silke.zimmermann@medizin.uni-leipzig.de

Running head: Noncanonical microglial IL-1β maturation in CKD

GRAPHICAL ABSTRACT

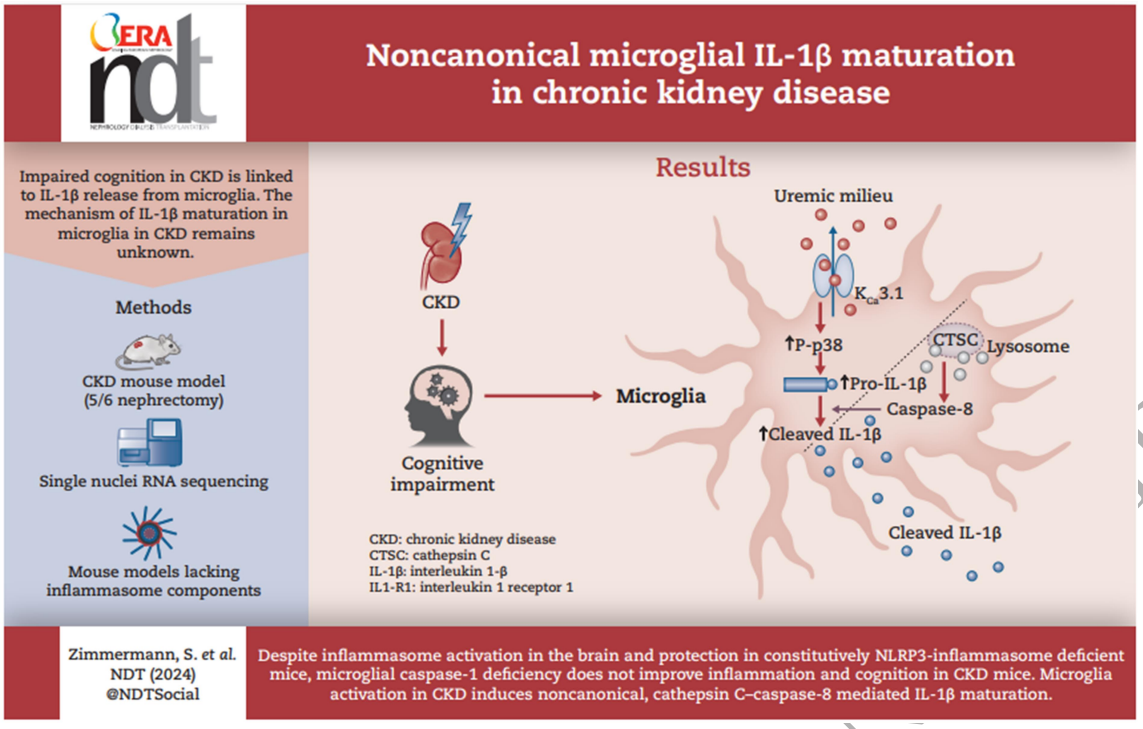

ABSTRACT

Background and hypothesis.

Organ transplantation reverses cognitive impairment in chronic kidney disease (CKD), indicating that cognitive impairment driven by CKD is therapeutically amendable. We recently demonstrated that impaired cognition in CKD is linked to IL-1β-release from microglia and IL-1R1-signaling in neuronal cells, thereby identifying a signaling pathway that can be exploited therapeutically. However, the mechanism of IL-1β-maturation in microglia in CKD remains unknown. We hypothesized that microglia cells require caspase-1 for CKD-driven cognitive impairment.

Methods.

We used a combination of single cell analyses, *in situ* analyses, genetically modified mouse models (including newly generated Cre-LoxP mouse models) and *in vitro* models. The current study builds on a recently identified intercellular crosstalk between microglia and neurons that impairs cognition in chronic kidney disease (CKD).

Results.

Here, we show that despite NLRP3 inflammasome activation in the brain and protection of mice with constitutive NLRP3 deficiency from CKD-induced cognitive impairment, (i) caspase-1 is not required for IL-1β maturation in microglia and (ii) targeted caspase-1 deficiency in microglia does not improve cognition in CKD mice. These data indicate that IL-1β maturation in microglia is independent of the NLRP3-caspase-1 interaction in CKD. Indeed, microglia activation in CKD induces noncanonical, cathepsin C–caspase-8 mediated IL-1β maturation. Depletion of cathepsin C or caspase-8 blocks IL-1β maturation in microglia. Preliminary analyses suggest that noncanonical microglia IL-1β maturation occurs also in diabetes mellitus.

Conclusion.

These results identify a noncanonical IL-1β-maturation pathway as a potential therapeutic target to combat microglia-induced neuronal dysfunction in CKD and possible other peripheral diseases.

KEY LEARNING POINTS

What was known:

Although cognitive impairment is common in peripheral diseases such as chronic kidney disease (CKD), effective therapies are lacking. Kidney transplantation is able to reverse cognitive impairment, suggesting that CKD-induced cognitive impairment is therapeutically modifiable. However, the mechanisms underlying CKD-induced cognitive impairment remain largely elusive.

This study adds:

Here, we uncover a noncanonical pathway of IL-1β maturation in microglia, which is independent of caspase-1 and is mediated by cathepsin C – caspase-8. This indicates that strategies to prevent microglia IL-1β maturation without impeding the canonical NLRP3-caspase-1 inflammasome may be therapeutically feasible. This study thus provides new mechanistic insights into CKD-driven cognitive impairment.

Potential impact:

Considering that the NLRP3 inflammasome and IL-1R1 have crucial physiological functions, the noncanonical IL-1β maturation in microglia opens new possibilities for pharmaceutical interventions aiming to maintain cognition independent of the canonical NLRP3-inflammasome and IL-1R1. These insights are expected to motivate future studies, for example evaluating the relevance of cathepsin C – caspase-8 mediated IL-1β maturation in other diseases affecting cognition and developing approaches to inhibit this noncanonical IL-1β maturation pathway in microglia.

Keywords:

caspase-8, cathepsins, chronic diseases, cognition, inflammation, microglia signaling

INTRODUCTION

Although cognitive impairment is common in peripheral diseases such as chronic kidney disease (CKD), effective therapies are lacking[1–3]. Kidney transplantation is able to reverse cognitive impairment, reflecting that CKD-induced cognitive impairment is therapeutically modifiable[4–6]. However, the mechanisms underlying CKD-induced cognitive impairment

remain largely elusive. Microglia communicate with neurons and modulate their function[7], both conveying detrimental or beneficial effects[8], in part via cytokines[9–13]. Sterile inflammation via inflammasome signaling is a common trait of peripheral diseases associated with cognitive impairment, such as in CKD[14–16]. Sterile inflammation is not limited to the peripheral organs, as reflected by reports of NF-κB p65 activation (increased nuclear translocation) and elevation of pro-oxidant and pro-inflammatory mediators in the brain in the context of CKD[17]. Using a mouse model of chronic kidney disease (CKD, 5/6 nephrectomy), we recently demonstrated that activation of microglia in CKD is associated with potassium efflux and IL-1β release, which impairs cognition[18]. CKD mice with neuron-specific loss of IL-1R1 were protected from CKD-induced cognitive impairment, suggesting a microglia-neuron cross-talk via IL-1β released from microglia and acting on IL-1R1 expressed by neurons[18]. However, the mechanism of IL-1β maturation in microglia remain unknown.

Several studies demonstrated that neurodegenerative processes are ameliorated in mice with a constitutive NLRP3-deficiency. Based on these studies, further *in vitro* studies and conceptual consideration, it is generally assumed that the NLRP3 – caspase-1 – inflammasome is activated in microglia, promoting IL-1β release from microglia. However, a limitation of these pre-clinical studies was the use of mice with a constitutive deficiency of components of the NLRP3-caspase-1 inflammasome[14]. Thus, while these studies provided important insights into neurodegenerative disease processes, they did not identify the relevant cell types in which the NLRP3 inflammasome is activated or evaluate the involvement of other mechanisms of IL-1β maturation in specific brain cells. Considering different inflammasomes and noncanonical pathways leading to IL-1β maturation, identification of cell-specific IL-1β maturation pathways may identify possible new therapeutic approaches to CKD-associated cognitive impairment. In the CKD model, the priming step of IL-1β activation depends on potassium efflux from and p38-activation in microglia[18]. Yet, it remains unknown whether microglial IL-1β maturation in CKD mice depends on NLRP3, another inflammasome or an unrelated mechanism. Defining the mechanism of IL-1β maturation in microglia may identify new therapeutic approaches to combat CKD-induced cognitive impairment.

MATERIALS AND METHODS

Cell culture

Immortalized murine microglia cells (SIM-A9, ATCC CRL-3265™) and murine neuronal cells (Neuro-2, Cell lines service, 400394) were maintained at 37°C in cell culture media (microglia: DMEM-F12, 10 % heat inactivated FBS, 5 % heat inactivated horse serum; neurons: EMEM, 10 % FBS). For experiments, neuronal cells were serum-starved (2 % FBS) for 5 days prior to the experiment in order to induce differentiation. Casp1 and Casp8 knock out murine microglia cells were generated by transfecting cells with Casp1 or Casp8 CRISPR/Cas9 KO plasmid (Santa Cruz). After 24 h, transfected cells were sorted, and GFP-positive single cells were sorted in 96-well plates. Single cell clones were expanded and screened for knock out by immunoblotting. Cell lines were routinely tested negative for mycoplasma. Cells were cultured in 10 cm^2 dishes and treated as follows: microglia were incubated for 6 h with stimuli (10 % control plasma, 10 % CKD plasma, or LPS (in addition to the standard 10 % FBS and 5 % horse serum), followed by removal of medium, adding of fresh medium and further incubation for 12 h to generate conditioned medium (CM). The CM was harvested, centrifuged at 300 g for 5 min and the supernatant added to the neuronal cells for a period of 24 h. As previously shown[18], human control plasma had no effect, indicating that an unspecific effect of human plasma per se can be largely excluded.

Mice

Wild-type mice (C57BL/6, age 6-8 weeks) were obtained from Janvier Lab (S.A.S., St. Berthevin Cedex, France). $NLRP3^{-/-}$ mice have been described before[20,21]. Mice had been backcrossed onto the C57Bl/6 background for at least 9 generations. Non-diabetic C57BLKsJ-db/+ (db/m) and diabetic C57BL/KSJ-db (db/db) male and female mice were obtained from Janvier (S.A.S., St. Berthevin Cedex, France). All animal experiments were conducted according to standards and procedures approved by the local Animal Care and Use Committee (Landesverwaltungsamt Halle and Landesverwaltungsamt Leipzig, Germany). Animal care and treatment were conducted in conformity with institutional guidelines that are in compliance with international laws and politics. The permission of the animal protection commission was given.

We generated new mouse models. In detail, we obtained ES-cells from Eucomm containing mutant caspase-1 genes with the potential to generate conditional knock-out mice using the

Cre-LoxP approach. These ES-cells were successfully injected into oocytes, giving rise to founder mouse lines. Founder mice were identified using complimentary PCR-strategies analysing the 5'-, 3'- and middle region of the targeted gene locus (representative PCRs shown in Supplementary Fig. S2, tail DNA was used for genotyping by PCR; primers, see Table S1). Confirmed founder mice were crossed with ubiquitously expressing flippase mice (ubiquitously expressing an enhanced variant of Saccharomyces cerevisiae FLP1 recombinase under the control of the human β-actin promoter (transgenic B6.Cg-Tg[ACTFlpE]9205Dym/J mice obtained from Jackson Laboratories)) to delete the LacZ-Stop sequence. After genetic deletion of the LacZ-Stop sequence (which conveys a complete knock out) we obtained conditional knock out mice for caspase-1 (caspase-1^{LoxP}), which were again identified by PCR. These mice were crossed with $Cx3Cr1^{Cre}$ (microglia Cre-expression) mice to generate mice with cell-type specific loss of caspase-1.

CKD mouse model (5/6 nephrectomy model)

To mimic chronic renal failure with uremia in mice, we conducted 5/6 nephrectomy (NX), as described before[18]. 5/6 nephrectomy was induced in a two-step surgical procedure: (i) ablation of 2/3 of the renal parenchyma of the right kidney in 6 to 8 weeks old mice, (ii) followed 7 days later by complete nephrectomy of the contralateral kidney (5/6 NX). Mice were randomly allocated to 5/6 NX or sham operation (identical procedure without removing kidney parenchyma). Mice were operated under Ketamine (25mg/ml)/Xylocaine (2%) anesthesia (mixture of 1850ml Ketamine plus 150ml Xylocaine, 70µL/mouse intraperitoneally). In detail, mice were placed on a disinfected, heated surgery desk, the skin was disinfected, and eyes were protected with Vidisic® (Carbomer 980: 2 mg pro Gramm) 10 g against dehydration. A ventral midline incision into the abdomen was made to expose the animal's right kidney. The intestines were mobilized and placed extracorporeally embedded in humid tissue to avoid dehydration. The kidney was mobilized and carefully decapsulated, leaving the adrenal gland intact and in situ. A surgical suture is placed and ligated around each pole of the kidney, leaving 1/3 of the middle kidney intact. The kidney tissue distal to the ligature (the kidney poles) were excised and the abdominal incision was closed after ensuring hemostasis of the surgical sites. In the second surgery, 7 days after the first surgery, the animal was placed as described before and the first wound sutures placed after the first surgery were removed to open the abdominal cavity. The left kidney was

mobilized and the renal vessels were isolated and ligated with a suture. With a second suture we isolate and ligate the ureter to avoid leakage of urine in the abdominal cavity after surgery. Vessels and the ureter were cut distally to the ligations. The left kidney is taken out and the abdominal incision was closed after ensuring hemostasis. The average surgery time was 10-15 minutes. Impaired renal function mimicking chronic renal failure was ascertained six weeks post the second surgery by demonstrating increase of urea and creatinine.

6 weeks post-surgery, the body weight was measured, and mice were sacrificed. Blood samples were obtained from the inferior vena cava of anticoagulated mice (500 U of unfractionated heparin, 50 µL volume, in the vena cava directly before blood collection)[20,22–26]. Blood was centrifuged at 2000 × g for 20 min at 4°C, and plasma was snap-frozen in liquid nitrogen. Mice were perfused with ice-cold PBS for 10 min for immunofluorescence analyses, RNA or protein isolation or further perfused with 4% buffered paraformaldehyde[20,22–26] for immunohistochemistry analyses. Paraformaldehyde-perfused tissues were further fixed in 4% buffered paraformaldehyde for 24 h, embedded in paraffin and processed for sectioning.

Histology and immunohistochemical analysis

Described in the Supplements

snRNA-Seq

For experiments utilizing the 10x Genomics platform, the following reagents were used: Chromium Next GEM Single Cell 3' Library kit v3.1 (PN-1000158), Chromium Next GEM Single Cell 3' GEM Kit v3.1 (PN-1000130), Chromium Next GEM Single Cell 3' Gel Bead Kit v3.1 (PN-1000129) and Dynabeads MyOne SILANE (PN-2000048) and were used according to the manufacturer's instructions in the Chromium Single Cell 3' Reagents Kits V3.1 User Guide. Single nuclei droplets were generated using 10X Genomics Droplet generator and in total 10,000 nuclei per sample were targeted.

Sequencing and read mapping: Generated libraries were sequenced on an Illumina NextSeq 500 at the Next Generation Sequencing Facility[ZS1] of the Max Planck Institute of Biochemistry with >50 x 10^3 reads per nucleus followed by de-multiplexing and mapping to the mouse genome (build mm10) using CellRanger v3.0 (10x Genomics) with standard settings and inclusion of introns for nuclear transcripts. Count matrixes were further analyzed with Seurat V3.1.4 R package [27]. Data was filtered by removing low expressed

genes and low-quality nuclei from further analyses: (i) genes with 0 raw counts were removed; (ii) nuclei with <600 uniquely expressed genes were excluded; (iii) nuclei with high percentage of mitochondrial genes (>5%) were removed. The data were normalized using the *NormalizeData()* function, the 2000 most variable features detected with *FindVariableFeatures()*, data scaled with *ScaleData()*, the first 30 principal components calculated with *RunPCA()*, and used for clustering (*RunUMAP(), FindNeighbours(), FindClusters()*). Doublets were removed with the DoubletFinder R package according to the doublet rates provided by 10x Genomics. Next, cell types and identities were assigned to Seurat clusters based on the co-expression of multiple marker genes (neurons (Tubb3, Mef2c); neuronal precursors (Gad1 and Neurod2); astrocytes (Aldh1l1 and Gfap); oligodendrocytes (Olig1, Plp1, Mbp, Mog); vascular cells (Pecam1, Cd34, Rgs5); monocytes (Fcgr3a), T-cells (Foxp3, Cd3e), microglia (Ptprc, C1qa, Ctss, Aif1, Itgam, P2ry12). Differentially expressed genes between clusters and conditions were obtained using the *FindMarkers()* function based on a Wilcoxon Rank Sum test with Benjamini p-value correction. Genes were considered differentially expressed based on fold change, minimum expression and adjusted *P* value cut-offs of ($p < 0.05$). Raw data from the scRNA-seq analyses have been uploaded to the GEO under the accession number GSE218613.

Statistical Analysis

Mice were grouped according to genotype, and randomly assigned to different interventions (sham, nephrectomy, TRAM34). Data are summarized as the mean ± standard error of the mean (SEM). Statistical analyses were performed with Student's t test or one-way ANOVA, as appropriate, and indicated in the figure legends. Post-hoc comparisons of ANOVA were corrected with the method of Dunnett multiple comparison. The Kolmogorov–Smirnov test or D'Agostino-Pearson normality test was used to determine whether the data were consistent with a Gaussian distribution. Prism 8 (www.graphpad.com, accessed on 3rd August 2022) software was used for statistical analyses. Values of $p \leq 0.05$ were considered statistically significant. Statistical analyses are mentioned in the Data Supplement for analyses of RNAseq data and in the corresponding figure legends.

RESULTS

Microglia activation in CKD is independent of NLRP3

In a model of CKD, we recently established that levels of activated (cleaved) caspase-1 and IL-1β proteins were increased in the cortices of CKD versus control mice[18]. These data suggest NLRP3 inflammasome activation in the brain in the context of CKD. To determine the relevance of the NLRP3 inflammasome, we compared mice with constitutive *Nlrp3*-deficiency (*NLRP3*^{KO}) mice to wild-type (*NLRP3*^{Cont}) mice. CKD was induced in a subgroup of mice by 5/6 nephrectomy (**Figure 1a**), which increased serum urea and creatinine in both genotypes to a comparable extent (**Figure 1b**). In agreement with our recent report, CKD reduced neuronal K^+ turnover, as reflected by TlAMG, indicating reduced neuronal activity, while K^+ turnover was increased in microglia cells, reflecting increased microglia activation in wild-type mice. In mice lacking NLRP3 (CKD NLRP3^{KO} mice), reduced neuronal K^+ turnover was normalized (**Figure 1c, d**), which was associated with improved memory function (**Figure 1e, f**). While Tl^+ uptake was normalized in neurons, Tl^+ uptake was persistently increased in microglia. These observations indicate (i) that constitutive full-body *Nlrp3*-deficiency is sufficient to improve neuronal function, as reflected by neuronal K^+ turnover and improved memory function, and (ii) microglial activation persists in NLRP3$^{-/-}$ CKD mice, indicating that microglia potassium efflux and activation is independent of NRLP3 (**Figure 1c, d**).This observation supports a model in which CKD induces potassium efflux from microglia, which primes NLRP3-caspase-1 mediated IL-1β activation in microglia with subsequent effects on neurons. Conclusively, the unaltered K^+ turnover in microglia is congruent with our hypothesis, while the altered K^+ turnover in neurons indicates that the NLRP3 inflammasome does contribute to neuronal K^+ turnover "downstream" of noncanonical IL-1β maturation in microglia.

Microglial IL-1β maturation in CKD does not require caspase-1

To evaluate the role of the NLRP3-caspase-1 inflammasome specifically in microglia, we next conducted *in vitro* experiments. We exposed microglia to plasma obtained from individuals with normal kidney function (control plasma) or with CKD (CKD plasma, in both cases 10%

patient plasma plus 90% normal serum, see methods). Both, murine plasma and human plasma induced a comparable induction of cleaved IL-1β in murine and human microglia cell lines, respectively (**Supplementary Figure S1a, b**). Additionally, human plasma induces maturation of IL-1β in murine microglia cells[18]. Collectively, these data indicate that comparable results are obtained irrespectively whether human or mouse serum or plasma was used, allowing us to use readily available human plasma in experiments with human or mouse cells. While IL-1β mRNA was strongly induced in microglia upon stimulation with CKD plasma, Asc, Nlrp3 and Casp1 mRNA expression was not induced (**Figure 2a**), suggesting that CKD plasma primes IL-1β expression, but not expression of other components of the NLRP3 inflammasome. To verify this observation, we exposed microglia to control plasma, CKD plasma or LPS (positive control). CKD plasma failed to induce an NLRP3-ASC interaction in microglia, while LPS induced NLRP3-ASC interaction (**Supplementary Figure S1c, d**). These results suggest that microglia are capable of NLRP3 inflammasome activation, e.g. upon stimulation with LPS, but that stimulation with CKD plasma fails to do so. This finding suggests that microglial IL-1β maturation occurs independently of the NLRP3-caspase-1 inflammasome in CKD.

To scrutinize the dispensability of caspase-1 for IL-1β maturation in microglia stimulated with CKD plasma, we evaluated microglial lacking caspase-1 (**Supplementary Figure S1e, S2**). IL-1β release from microglia was increased upon exposure to CKD plasma, irrespective of caspase-1 expression (**Figure 2b**). This indicates microglia cells stimulated with CKD plasma induce IL-1β maturation, which, however, does not require caspase-1. This finding together with the above and our previous finding[18] suggest that microglia caspase-1 is not required for impaired cognition in CKD. To determine the dispensability of caspase-1 for CKD-induced impaired cognition, we generated mice lacking caspase-1 specifically in microglia ($Cx3cr1^{Cre}$ x $Casp1^{LoxP/LoxP}$ mice, referred to as $Casp1^{\Delta MC}$ mice; inactivation of caspase-1 expression was confirmed by immunofluorescence analysis (**Supplementary Figure S3a-f**). CKD was induced in a subgroup of mice by 5/6 nephrectomy (**Figure 2c**), which increased serum urea and creatinine in both genotypes to a comparable extent (**Figure 2d**). After 6 weeks of CKD, memory function was comparable in $Casp1^{\Delta MC}$ and $Casp1^{Cont}$ mice (**Figure 2e, f**), corroborating that microglial caspase-1 is dispensable for the induction impaired cognition in CKD mice.

Caspase-8 mediates CKD-induced IL-1β cleavage in microglia

To gain insights into potential mechanisms mediating CKD-dependent IL-1β cleavage in microglia, we reanalyzed snRNAseq data obtained from brains of control and CKD mice[18]. Biological process analysis revealed a role of immune response and inflammation in the microglia cluster in CKD (**Figure 3a**). Consistent with caspase-1-independent IL-1β maturation in microglia in CKD conditions, caspase-1 expression was not induced in the microglial cluster, while pro-IL-1β expression was increased 2.7-fold (**Figure 3b**). In contrast to caspase-1, the expression of caspase-8, which has been linked to microglial inflammasome activation and neuroinflammation[18], was increased 1.4-fold (**Figure 3b, c**), raising the question as to whether microglial caspase-8 contributes to CKD-induced IL-1β maturation in microglia. To scrutinize this possibility, we compared control (ctrl) and caspase-1 ($Casp1^{KO}$) versus caspase-8 ($Casp8^{KO}$)-deficient microglia cells stimulated with CKD plasma. CKD plasma induced IL-1β cleavage in $Casp1^{Cont}$ and $Casp1^{KO}$ but not $Casp8^{KO}$ microglial (**Figure 2b, 3d; Supplementary Figure S2**), demonstrating that caspase-8 is required for IL-1β maturation in microglia stimulated with CKD plasma.

We have previously shown that under CKD-conditions IL-1β released from microglia induces potassium dyshomeostasis in neurons, reflecting neuronal dysfunction[18]. To determine whether reduced neuronal potassium efflux depends on caspase-8 in microglia, we cultured control, $Casp1^{KO}$, and $Casp8^{KO}$ microglia cells with CKD plasma, generating conditioned medium (CM^{CKD}). Neurons were then exposed to this CM^{CKD} and K^+ turnover in neurons was determined by staining for the potassium analogion Tl^+, which is taken up by neurons in exchange for potassium released due to neuronal activation. While CM^{CKD} obtained from $Casp^{Cont}$ or $Casp1^{KO}$ microglial cells impaired K^+ turnover, CM^{CKD} obtained from $Casp8^{KO}$ microglial cells had no effect (**Figure 3e, f; Supplementary Figure S2**). Together with our recent results[18], these observations support a model in which caspase-8 promotes microglial IL-1β maturation, which in turns impairs Tl^+ turnover in neurons and hence neuronal potassium turnover and function.

Lysosomal cathepsin C promotes microglia caspase-8 activation

We next addressed the question how caspase-8 dependent IL-1β maturation may be induced by CKD-plasma independent of caspase-1. Caspase-1 independent pathways of IL-1β

maturation have been reported, including cathepsin C dependent mechanisms[28–30]. In microglial cells of CKD mice, genes related to lysosomes were the most differentially regulated genes upon KEGG pathway analyses, with cathepsin C (CTSC) being the most strongly induced gene (**Figure 4a**). CTSC expression was readily detected in microglia but not in neurons, and CTSC activity was induced in microglia exposed to CKD plasma (**Figure 4b, Supplementary Figure S4a, b**). Hence, we speculated that CTSC induces IL-1β maturation in microglia cells stimulated with CKD plasma. To determine whether microglial noncanonical IL-1β maturation as described above is specific for CKD conditions or may be observed in other disease settings, we determined whether CTSC is induced in another chronic disease, diabetes mellitus. In brain tissue of diabetic mice (db/db, 24 weeks old, **Supplementary Figure S5c, d**), induction of CTSC expression and of cleaved IL-1β was readily detectable and of similar magnitude as in brains of CKD mice (**Figure 4c-e**). These data indicate that the identified pathway is not specific for CKD but may be also relevant in other peripheral diseases such as diabetes mellitus. Inhibition or knock down of *Ctsc* largely abolished caspase-8 activation in and IL-1β release from microglia cells stimulated with CKD plasma (**Figure 5a, b; Supplementary Figure S4e**). Of note, markers of microglia activation, such as IBA1 expression and microglia soma width, were also reduced upon *Ctsc* knock down (**Figure 5c-e; Supplementary Figure S4e**), indicating that CTSC inhibition prevents microglial activation by CKD plasma. These data imply that cathepsin C is activated in CKD conditions and induces microglial caspase-8 activation and IL-1β maturation.

DISCUSSION

We recently established that in CKD conditions, IL-1β secreted from microglia leads to IL-1R1-mediated neuronal signaling that impairs cognition[18]. Given available data[18,31–33], we hypothesized that IL-1β maturation in microglia in CKD depends on the NLRP3 inflammasome and caspase-1 activation. Contradictory to this hypothesis, our data establish that – at least in CKD – IL-1β maturation in microglia is independent of caspase-1. We identify here a multi-step, noncanonical process of inflammasome activation, which depends on MAPK-signaling[18] and activation of cathepsin C and caspase-8. This multi-step process allows tight regulation of IL-1β maturation in microglia, which is characteristic for cells of the innate immune system[34].

Our analyses indicate that the same noncanonical, NLRP3-independent pathway may be activated in diabetes mellitus, suggesting that cathepsin C – caspase-8 mediated IL-1β maturation in microglia is not specific for CKD. Renal impairment in the db/db model results in a roughly two-fold creatinine-increase at the age of 24 weeks, similar to the increase observed in the CKD mice. In complex conditions like diabetes mellitus, additional factors such as metabolic alterations or obesity-related adipokine may contribute to a cognitive decline. The 5/6 nephrectomy CKD model is particularly valuable because it enables to study the impact of impaired renal function in the absence of an underlying diseases, highlighting that renal dysfunction per se can drive cognitive impairment.

The identification of a noncanonical IL-1β maturation pathway in microglia may unravel new therapeutic options, considering that the canonical NLRP3 inflammasome and IL-1R1 have crucial physiological functions. Indeed, in the CANTOS trial which evaluated canakinumab in patients at risk of myocardial infarction, canakinumab increased the risk of infection[35]. Targeting the noncanonical IL-1β maturation in microglia is not expected to interfere with the canonical inflammasome and is hence not expected to induce unwanted side-effects, such as an increased risk of inflammation. Hence, targeting noncanonical inflammasome activation may open new possibilities for pharmaceutical interventions to maintain cognition while reducing the risk of side-effects.

Along this line, we recently demonstrated that the calcium-activated potassium channel $K_{Ca}3.1$, which is predominately expressed by microglia[36,37], mediates potassium efflux from and activation of microglia cells[37,38]. Inhibition of $K_{Ca}3.1$ was sufficient to protect CKD mice from neuronal potassium dyshomeostasis and impaired cognition[18], illustrating that the identification of cell- and context-specific activation mechanism may uncover new therapeutic approaches allowing to target a subgroup of patients. Future studies are required to validate the relevance of the proposed mechanisms in diseases other than CKD and to evaluate possible therapeutic approaches.

Distinctive pathways leading to IL-1β maturation have been reported before. Thus, different caspases mediate IL-1β maturation in peripheral macrophages and microglia cells, e.g. caspase-1, -4, and -5 in macrophages, but caspase-3/7 or caspase-8 in microglia[39,40]. The current data support that IL-1β maturation in microglial cells is independent of caspase-1 but dependent on cathepsin C and caspase-8, at least in the setting of CKD. Different

mechanisms of IL-1β maturation in peripheral macrophages and microglia may reflect their disjunct ontogeny, as microglia originate from the yolk sac while peripheral macrophages are bone-marrow derived[41]. The engagement of different signaling pathways controlling comparative effects (here: IL-1β maturation) may allow therapeutic approaches specifically targeting subpopulations of cells, for example, macrophages versus microglia.

Previous studies suggested a role of the canonical NLRP3-Casp1 inflammasome in neurodegenerative diseases and in microglia cell activation[15]. At face value our results appear to contradict these results. The apparently different results may reflect the different models and approaches used, as most studies analyzing a role of the NLRP3 inflammasome in microglia cells used *in vitro* models, which are always at least to some extent artificial, or *ex vivo* analyses of constitutive *Nlrp3*-deficient mice[14]. The use of constitutively NLRP3-deficient mice obviously precludes the identification of relevant cell types in which the NLRP3 – caspase-1 inflammasome is required. The use of mice with cell-specific (CX3CR1-dependent) inhibition of caspase-1 in microglia in the current study revealed that caspase-1 is dispensable for neuronal dysfunction and cognitive impairment at least in the CKD model. Notably, the chosen approach to inactivate caspase-1 also deletes caspase-1 from CX3CR1-expressing macrophages. Hence, the failure of CX3CR1-dependent caspase-1 inactivation to improve cognition supports the notion that caspase-1 in any CX3CR1-expressing cell type (e.g. microglia and macrophages) does not contribute to impaired cognition in CKD.

The divergence between our analyses showing the importance of caspase-8 versus caspase-1[15] may also reflect context-specific mechanisms of IL-1β processing in microglia. While in our hands, CKD-derived plasma failed to induce canonical NLRP3-caspase-1 inflammasome activation, LPS, used as a positive control, readily activated the canonical NLRP3-Casp1 inflammasome and induced IL-1β maturation in microglia, corroborating results of previous reports[42,43]. These observations support that different pathways induce microglial IL-1β maturation. These pathways may be independently activated in a context-specific fashion or may act synergistically, as previously proposed[28]. At the same time, the engagement of distinct pathways leading to IL-1β maturation may allow inhibition of CKD-associated neuro-inflammation without impairing microglial IL-1β maturation and release upon other disease stimuli, such as LPS.

An interesting observation in the current study is the protection of constitutively NLRP3-deficient or constitutively caspase-1-deficient mice, but not of mice lacking caspase-1 specifically in microglia. While this observation provides strong evidence that the canonical NLRP3-caspase-1 pathway is not required in microglia for CKD-induced neuronal dysfunction and impaired cognition, it nevertheless indicates a crucial function of the canonical NLRP3–caspase-1 pathway in cells other than microglia. Whether the latter indicates a possible new function of NLRP3 in neurons or an interaction of neurons not only with microglia, but also with an additional cell type expressing NLRP3 (such as astrocytes or glia cells) remains to be established. This is entirely congruent with previous reports reporting protection of constitutively NLRP3- or caspase-1-deficient mice[14]. It is possible that noncanonically matured IL-1β released from microglia activates other cells such as vascular cells or astrocytes. These cells, once activated by IL-1β, may generate more IL-1β via the canonical NLRP3–caspase-1 pathway, thus aggravating the disease process. The results of our snRNAseq data in the vascular cell cluster indeed suggest that the NLPR3-caspase-1 inflammasome may be activated in these cells. It remains to be shown whether inhibiting noncanonical IL-1β maturation in microglia has an impact on the NLRP3 inflammasome in other brain cells and is thus sufficient to prevent or stop the impaired neuronal function. The latter appears possible, as inhibiting the potassium channel $K_{Ca}3.1$, which is predominately expressed by microglia[36,37], is sufficient to protect CKD mice from impaired cognition[18].

Another possible explanation for the protection observed in mice constitutively lacking NLRP3 or caspase-1 are noncanonical effects of NLRP3 or caspase-1. Noncanonical functions of NLRP3 have been reported. For example, NLRP3 acts as a transcriptional co-factor in T-cells or as an inducer of TGFβ-dependent renal injury[44,45]. Whether such noncanonical effects of NLRP3 contribute to impaired cognition and thus explain the neuroprotective effect observed in mice with a constitutive deficiency of NLRP3 remains to be shown.

The current study has some limitations. We provide evidence that the identified cathepsin C – caspase-8 dependent mechanism of IL-1β maturation in microglia may be relevant in diabetes mellitus, another peripheral disease. Yet, stringent evidence supporting a role of the noncanonical IL-1β maturation pathway identified here in other peripheral diseases is lacking and requires further experimental work. Furthermore, while we use targeted gene-inactivation of caspase-1 in microglia to show its dispensability for CKD-induced impaired cognition, we do not prove *in vivo* that the proposed cathepsin C – caspase-8 dependent

mechanism is required in microglia. Studies using targeted gene-inactivation of cathepsin C or caspase-8 are required to address this in the future. Next, while the conducted studies did not specifically investigate possible structural changes such as demyelination and microthrombosis, the mouse brains appeared macroscopically and microscopically normal. However, future studies are required to evaluate potential ultrastructural changes. Lastly, while the behavioural tests used are well established and provide important information and a robust phenotype in the CKD mouse model, we acknowledge that additional behavioural test may bolster the conclusion.

In this study, we did not seek to identify a single uremic toxin as the cause of cognitive impairment in CKD. Given the extensive range of uremic toxins, we assumed that a cognitive decline probably results from a combination of uremic toxins. Therefore, targeting just one toxin would likely be insufficient to address the medical problem. Instead, our focus was to identify a common or unifying mechanism in the brain impairing cognition in CKD. We hypothesized that targeting such central mechanism may improve cognition in CKD, regardless of the variety of uremic toxins involved. Our results, at least in the mouse model used, support this hypothesis. Together with our previous report, demonstrating that inhibition of the potassium channel $K_{Ca}3.1$ or of IL-1R signaling targets CKD-induced cognitive impairment[18], these results indicate several possible therapeutic approaches which can be validated in future pre-clinical and possibly clinical studies.

DATA AVAILABILITY STATEMENT

All data are available in the main text or the supplementary materials.

ACKNOWLEDGEMENTS

We thank Kathrin Deneser, Rumiya Makarova, Raik Rönicke, Susanne von Kenne and Monika Riek-Burchardt for excellent technical support and Prof. Dr. Marc Schönwiesner for his support.

FUNDING

Deutsche Forschungsgemeinschaft (DFG, German Research Foundation): IS-67/22-1, IS-67/25-1, IS-67/26-1, SFB854/B26, 361210922/GRK2408/P7&P9 (BI)

DFG grant 457240345 (BS)

DAAD scholarships (AE)

Medical Faculty of the University of Leipzig

AUTHORS' CONTRIBUTIONS

Conceptualization: SZ, BI

Methodology: SZ, AM, OB, JG, IB

Investigation: SZ, AM, AE, SJ, RR

Visualization: SZ

snRNA-seq analyses: SZ, OB, BS

Funding acquisition: SZ, BI, BS, AE

Project administration: BI

Supervision: BI, BS

Writing – original draft: SZ, BI

Writing – review & editing: SZ, BI, AM, OB, BS, RR, AE, JG

CONFLICT OF INTEREST STATEMENT

The authors report no competing interests.

REFERENCES

1. Drew, D. A., Weiner, D. E. & Sarnak, M. J. Cognitive Impairment in CKD: Pathophysiology, Management, and Prevention. *American journal of kidney diseases : the official journal of the National Kidney Foundation* **74,** 782–790; 10.1053/j.ajkd.2019.05.017 (2019).
2. Kachaamy, T. & Bajaj, J. S. Diet and cognition in chronic liver disease. *Current opinion in gastroenterology* **27,** 174–179; 10.1097/MOG.0b013e3283409c25 (2011).
3. Kurella, M., Chertow, G. M., Luan, J. & Yaffe, K. Cognitive impairment in chronic kidney disease. *Journal of the American Geriatrics Society* **52,** 1863–1869; 10.1111/j.1532-5415.2004.52508.x (2004).
4. Radić, J. *et al.* Kidney transplantation improves cognitive and psychomotor functions in adult hemodialysis patients. *American journal of nephrology* **34,** 399–406; 10.1159/000330849 (2011).
5. van Sandwijk, M. S. *et al.* Cognitive Improvement After Kidney Transplantation Is Associated With Structural and Functional Changes on MRI. *Transplantation Direct* **6**; 10.1097/TXD.0000000000000976 (2020).
6. Pantiga, C., Rodrigo, L. R., Cuesta, M., Lopez, L. & Arias, J. L. Cognitive deficits in patients with hepatic cirrhosis and in liver transplant recipients. *The Journal of neuropsychiatry and clinical neurosciences* **15,** 84–89; 10.1176/jnp.15.1.84 (2003).
7. Cserép, C. *et al.* Microglia monitor and protect neuronal function through specialized somatic purinergic junctions. *Science (New York, N.Y.)* **367,** 528–537; 10.1126/science.aax6752 (2020).
8. Viviani, B., Boraso, M., Marchetti, N. & Marinovich, M. Perspectives on neuroinflammation and excitotoxicity: a neurotoxic conspiracy? *Neurotoxicology* **43,** 10–20; 10.1016/j.neuro.2014.03.004 (2014).
9. Parkhurst, C. N. *et al.* Microglia promote learning-dependent synapse formation through brain-derived neurotrophic factor. *Cell* **155,** 1596–1609; 10.1016/j.cell.2013.11.030 (2013).
10. Shein, N. A. *et al.* Microglial involvement in neuroprotection following experimental traumatic brain injury in heat-acclimated mice. *Brain research* **1244,** 132–141; 10.1016/j.brainres.2008.09.032 (2008).
11. Hauptmann, J. *et al.* Interleukin-1 promotes autoimmune neuroinflammation by suppressing endothelial heme oxygenase-1 at the blood-brain barrier. *Acta Neuropathologica* **140,** 549–567; 10.1007/s00401-020-02187-x (2020).
12. Niu, L. *et al.* The critical role of the hippocampal NLRP3 inflammasome in social isolation-induced cognitive impairment in male mice. *Neurobiology of learning and memory* **175,** 107301; 10.1016/j.nlm.2020.107301 (2020).
13. Stoll, G., Jander, S. & Schroeter, M. Detrimental and beneficial effects of injury-induced inflammation and cytokine expression in the nervous system. *Advances in experimental medicine and biology* **513,** 87–113; 10.1007/978-1-4615-0123-7_3 (2002).

14. Heneka, M. T. *et al.* NLRP3 is activated in Alzheimer's disease and contributes to pathology in APP/PS1 mice. *Nature* **493,** 674–678; 10.1038/nature11729 (2013).

15. Heneka, M. T., McManus, R. M. & Latz, E. Inflammasome signalling in brain function and neurodegenerative disease. *Nature reviews. Neuroscience* **19,** 610–621; 10.1038/s41583-018-0055-7 (2018).

16. Butterworth, R. F. Hepatic Encephalopathy in Cirrhosis: Pathology and Pathophysiology. *Drugs* **79,** 17–21; 10.1007/s40265-018-1017-0 (2019).

17. Jing, W., Jabbari, B. & Vaziri, N. D. Uremia induces upregulation of cerebral tissue oxidative/inflammatory cascade, down-regulation of Nrf2 pathway and disruption of blood brain barrier. *American Journal of Translational Research* **10,** 2137–2147 (2018).

18. Zimmermann, S. *et al.* Chronic kidney disease leads to microglial potassium efflux and inflammasome activation in the brain. *Kidney international*; 10.1016/j.kint.2024.06.028 (2024).

19. Schubert, D., Humphreys, S., Vitry, F. de & Jacob, F. Induced differentiation of a neuroblastoma. *Developmental Biology* **25,** 514–546; 10.1016/0012-1606(71)90004-2 (1971).

20. Bock, F. *et al.* Activated protein C ameliorates diabetic nephropathy by epigenetically inhibiting the redox enzyme p66Shc. *Proceedings of the National Academy of Sciences of the United States of America* **110,** 648–653; 10.1073/pnas.1218667110 (2013).

21. Gross, O. *et al.* Syk kinase signalling couples to the Nlrp3 inflammasome for anti-fungal host defence. *Nature* **459,** 433–436; 10.1038/nature07965 (2009).

22. Madhusudhan, T. *et al.* Defective podocyte insulin signalling through p85-XBP1 promotes ATF6-dependent maladaptive ER-stress response in diabetic nephropathy. *Nature communications* **6,** 6496; 10.1038/ncomms7496 (2015).

23. Isermann, B. *et al.* Activated protein C protects against diabetic nephropathy by inhibiting endothelial and podocyte apoptosis. *Nature medicine* **13,** 1349–1358; 10.1038/nm1667 (2007).

24. Shahzad, K. *et al.* Stabilization of endogenous Nrf2 by minocycline protects against Nlrp3-inflammasome induced diabetic nephropathy. *Scientific reports* **6,** 34228; 10.1038/srep34228 (2016).

25. Shahzad, K. *et al.* Caspase-1, but Not Caspase-3, Promotes Diabetic Nephropathy. *Journal of the American Society of Nephrology : JASN* **27,** 2270–2275; 10.1681/ASN.2015060676 (2016).

26. Shahzad, K. *et al.* Nlrp3-inflammasome activation in non-myeloid-derived cells aggravates diabetic nephropathy. *Kidney international* **87,** 74–84; 10.1038/ki.2014.271 (2015).

27. Hao, Y. *et al.* Integrated analysis of multimodal single-cell data. *Cell* **184,** 3573-3587.e29; 10.1016/j.cell.2021.04.048 (2021).

28. Kono, H., Orlowski, G. M., Patel, Z. & Rock, K. L. The IL-1-dependent sterile inflammatory response has a substantial caspase-1-independent component that requires cathepsin C. *Journal of immunology (Baltimore, Md. : 1950)* **189,** 3734–3740; 10.4049/jimmunol.1200136 (2012).

29. Zhang, Y., Chen, Y., Zhang, Y., Li, P.-L. & Li, X. Contribution of cathepsin B-dependent Nlrp3 inflammasome activation to nicotine-induced endothelial barrier dysfunction. *European journal of pharmacology* **865,** 172795; 10.1016/j.ejphar.2019.172795 (2019).

30. Baumgartner, H. K. *et al.* Caspase-8-mediated apoptosis induced by oxidative stress is independent of the intrinsic pathway and dependent on cathepsins. *American journal of*

physiology. Gastrointestinal and liver physiology **293,** G296-307; 10.1152/ajpgi.00103.2007 (2007).

31. Ji, L., Jin, R.-J. & Li, L. Platelet-rich Plasma Improves Radiotherapy-induced Emotional Disorder and Cognitive Dysfunction, Neuroinflammation in Aged Rats by Inhibiting the Activation of NLRP3 Inflammasomes. *Neurochemical research* **48,** 2531–2541; 10.1007/s11064-023-03933-9 (2023).

32. Bai, H. *et al.* Cathepsin B links oxidative stress to the activation of NLRP3 inflammasome. *Experimental cell research* **362,** 180–187; 10.1016/j.yexcr.2017.11.015 (2018).

33. Halle, A. *et al.* The NALP3 inflammasome is involved in the innate immune response to amyloid-β. *Nature immunology* **9,** 857–865; 10.1038/ni.1636 (2008).

34. Schroder, K. & Tschopp, J. The inflammasomes. *Cell* **140,** 821–832; 10.1016/j.cell.2010.01.040 (2010).

35. Ridker, P. M. *et al.* Antiinflammatory Therapy with Canakinumab for Atherosclerotic Disease. *The New England journal of medicine* **377,** 1119–1131; 10.1056/NEJMoa1707914 (2017).

36. Maezawa, I., Jenkins, D. P., Jin, B. E. & Wulff, H. Microglial KCa3.1 Channels as a Potential Therapeutic Target for Alzheimer's Disease. *International journal of Alzheimer's disease* **2012,** 868972; 10.1155/2012/868972 (2012).

37. Lu, J., Dou, F. & Yu, Z. The potassium channel KCa3.1 represents a valid pharmacological target for microgliosis-induced neuronal impairment in a mouse model of Parkinson's disease. *Journal of neuroinflammation* **16**; 10.1186/s12974-019-1682-2 (2019).

38. Wulff, H. & Castle, N. A. Therapeutic potential of KCa3.1 blockers: recent advances and promising trends. *Expert review of clinical pharmacology* **3,** 385–396; 10.1586/ecp.10.11 (2010).

39. Burguillos, M. A. *et al.* Caspase signalling controls microglia activation and neurotoxicity. *Nature* **472,** 319–324; 10.1038/nature09788 (2011).

40. Burm, S. M. *et al.* Inflammasome-induced IL-1β secretion in microglia is characterized by delayed kinetics and is only partially dependent on inflammatory caspases. *The Journal of neuroscience : the official journal of the Society for Neuroscience* **35,** 678–687; 10.1523/JNEUROSCI.2510-14.2015 (2015).

41. Yang, J., Zhang, L., Yu, C., Yang, X.-F. & Wang, H. Monocyte and macrophage differentiation: circulation inflammatory monocyte as biomarker for inflammatory diseases. *Biomarker Research* **2,** 1; 10.1186/2050-7771-2-1 (2014).

42. Dutta, D., Liu, J., Xu, E. & Xiong, H. Methamphetamine Enhancement of HIV-1 gp120-Mediated NLRP3 Inflammasome Activation and Resultant Proinflammatory Responses in Rat Microglial Cultures. *International journal of molecular sciences* **25**; 10.3390/ijms25073588 (2024).

43. Rodrigues, F. d. S. *et al.* Cannabidiol prevents LPS-induced inflammation by inhibiting the NLRP3 inflammasome and iNOS activity in BV2 microglia cells via CB2 receptors and PPARγ. *Neurochemistry international* **177,** 105769; 10.1016/j.neuint.2024.105769 (2024).

44. Lorenz, G., Darisipudi, M. N. & Anders, H.-J. Canonical and non-canonical effects of the NLRP3 inflammasome in kidney inflammation and fibrosis. *Nephrology, dialysis, transplantation : official publication of the European Dialysis and Transplant Association - European Renal Association* **29,** 41–48; 10.1093/ndt/gft332 (2014).

45. Bruchard, M. *et al.* The receptor NLRP3 is a transcriptional regulator of TH2 differentiation. *Nature immunology* **16,** 859–870; 10.1038/ni.3202 (2015).

1

Fig.1

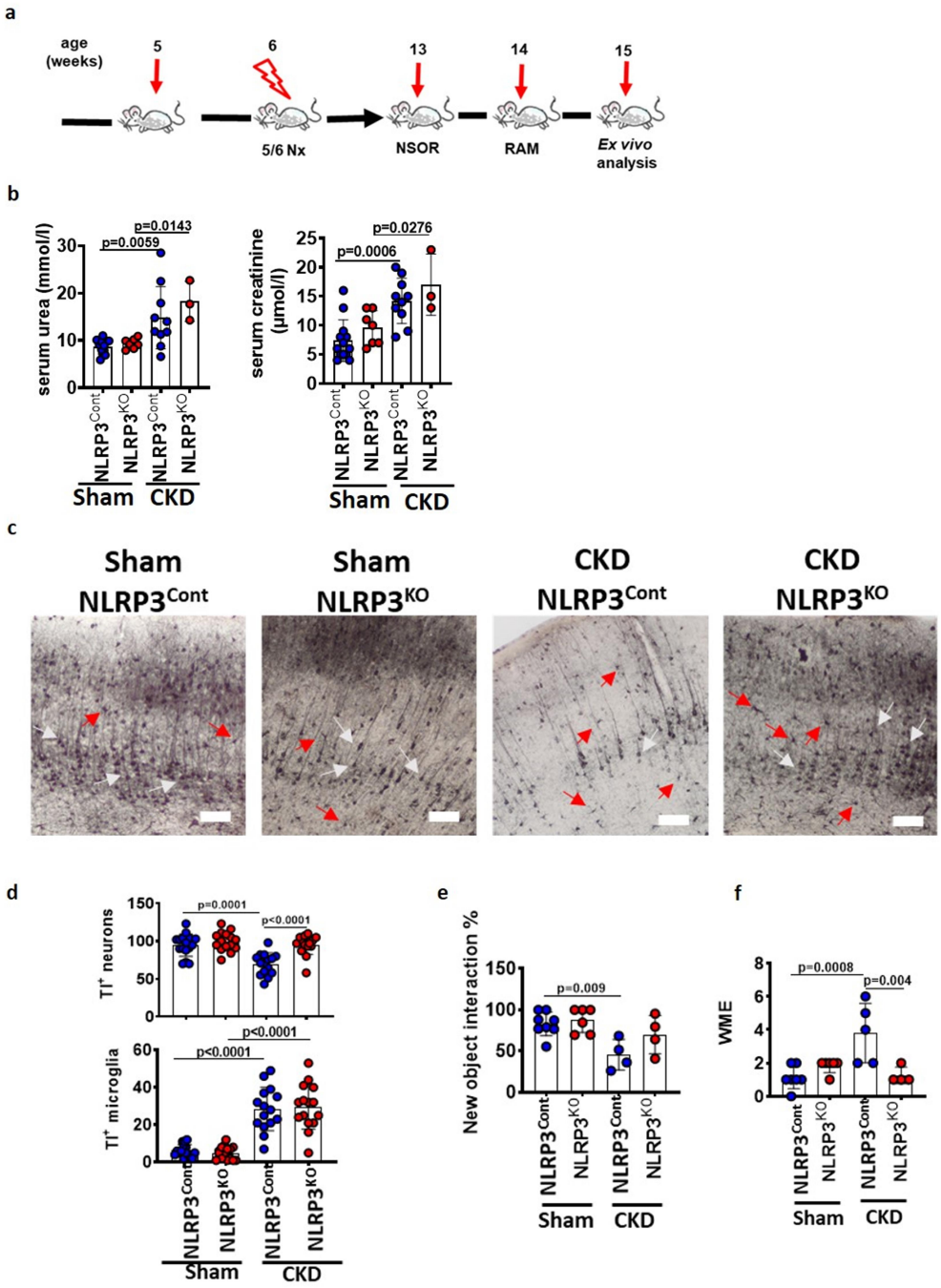

2

3 **Figure 1**

4 **Microglia activation in CKD is independent of NLRP3.** (**a**) Scheme summarizing the
5 experimental approach (5/6 nephrectomy, Nx) to induce CKD in mice and the timing of
6 behavioral assays and tissue harvest.

(**b**) Bar graphs (median ± SEM) summarizing renal retention parameters (urea and creatinine) 6 weeks post-surgery; *P* values: one-way ANOVA with Dunnett's post hoc comparison.

(**c, d**) Example images (**c**) and bar graph with dot plot (**d**, mean ± SEM, each dot represents data from one field of view) summarizing results for neurons (**d**, top) and microglia (**d**, bottom) of TlAMG stained cortices from wild-type (WT) and NLRP3-deficient ($NLRP3^{KO}$) sham and CKD mice. Red arrows depict microglia cells. White arrows depict neurons. Scale bar: 50 µm. *P* values: one-way ANOVA with Dunnett's post hoc comparison.

(**e, f**) Bar graph with dot plot summarizing the results of behavioral tests (**e**: NSOR, **f**: RAM) for WT CKD and $NLRP3^{KO}$ CKD mice. *P* values: one-way ANOVA with Dunnett's post hoc comparison. The data shown represent the mean ± SEM. NSOR = non-spatial object recognition, RAM = radial arm maze

Fig.2

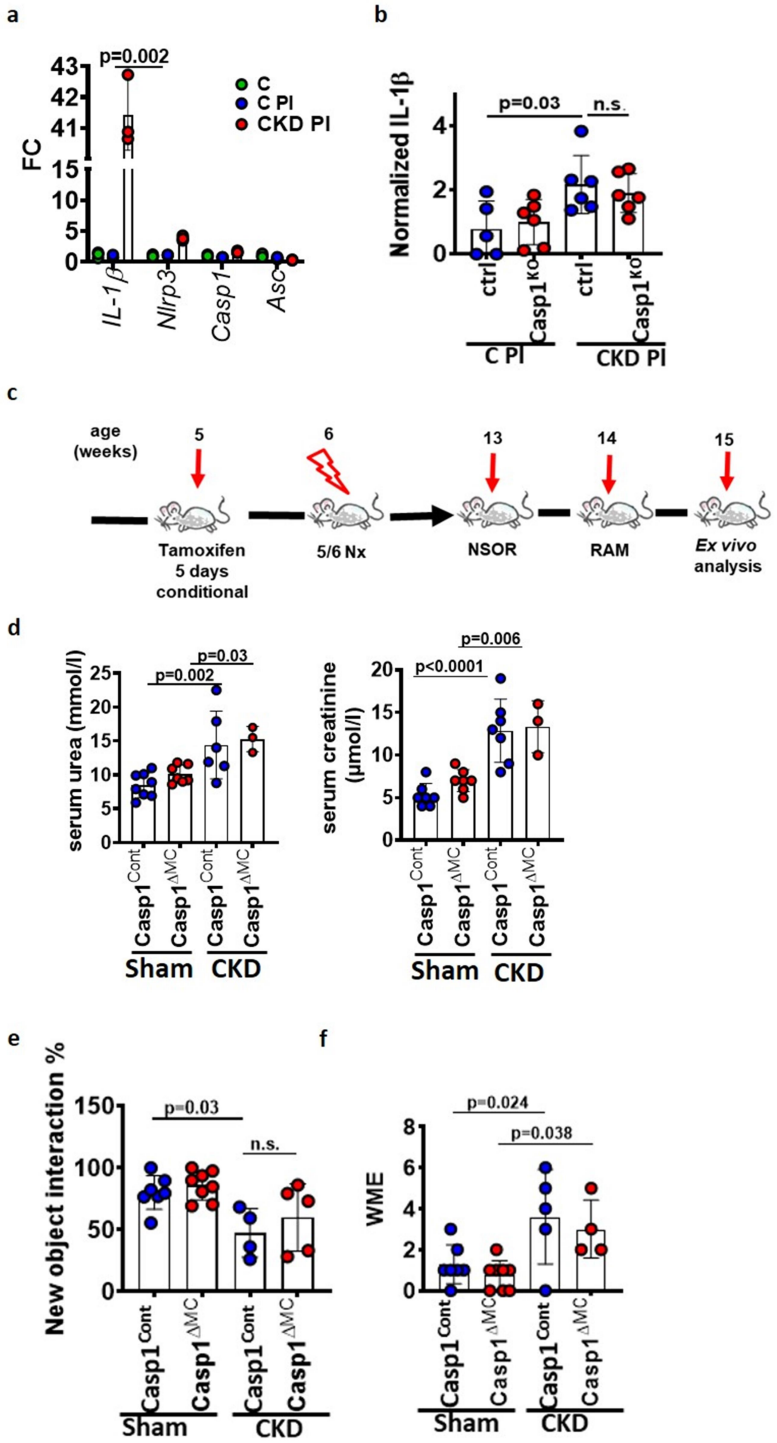

Figure 2

Microglial IL-1β maturation in CKD does not require caspase-1. (**a**) mRNA expression (fold change, FC; bar graph with dot plot, each dot represents one biological replicate) of *IL-1β*,

NLR family pyrin domain-containing 3 (*Nlrp3*), *Casp1* and adaptor molecule apoptosis-associated speck-like protein containing a CARD (*Asc*) in microglia exposed to control medium (C), control plasma (C Pl) or chronic kidney disease plasma (CKD Pl). *P* values were determined using one-way ANOVA with Dunnett's post hoc comparison.

(**b**) Bar graph with dot plot summarizing the IL-1β levels in the supernatant of microglia. WT and $Casp1^{KO}$ cells were exposed to control plasma (C Pl) or CKD plasma (CKD Pl). *P* values were determined using one-way ANOVA with Dunnett's post hoc comparison.

(**c**) Scheme summarizing the experimental approach (5/6 nephrectomy, Nx) to induce CKD in mice and the timing of behavioral assays and tissue harvest. Tamoxifen was injected to induce Cre recombinase, resulting in microglia-specific *Casp1* deficiency.

(**d**) Bar graphs (median ± SEM) summarizing renal retention parameters (urea and creatinine) 6 weeks post-surgery; *P* values: one-way ANOVA with Dunnett's post hoc comparison.

(**e, f**) Bar graphs with dot plots (each dot represents one mouse) reflecting cognition, as determined by nonspatial object recognition (NSOR, **d**; the results are reported as the frequency of time spent with the new unknown object) and radial arm maze (RAM, **e**; the results are reported as working memory errors, WMEs) tests in sham-operated control (sham) and CKD mice. Casp1 control ($Casp^{LoxP/LoxP}$) and $Casp1^{\Delta MC}$ mice (MC= microglial cell-specific deletion of caspase-1) were compared. *P* values were determined using one-way ANOVA with Dunnett's post hoc comparison.

Fig.3

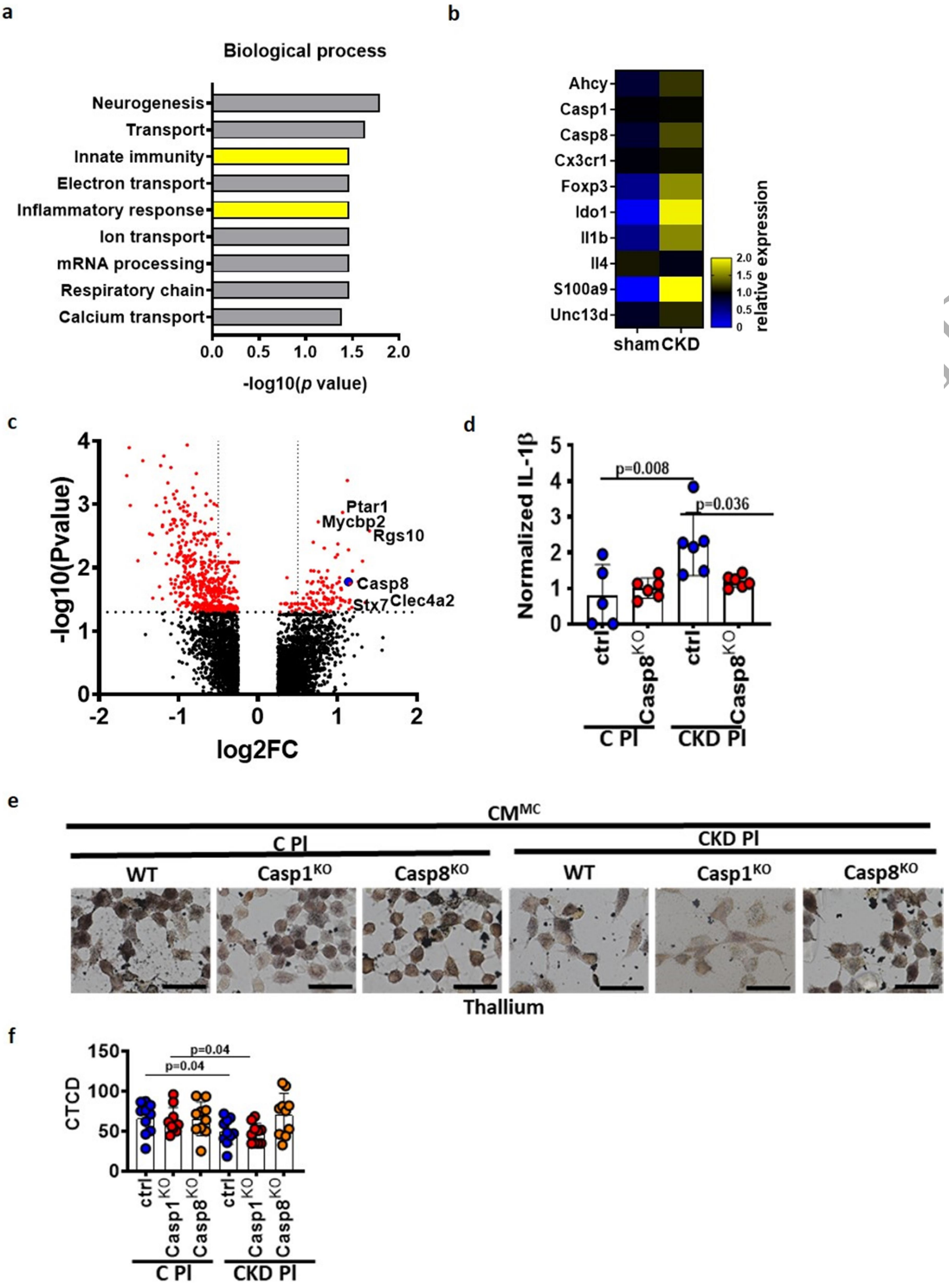

Figure 3

Caspase-8 mediates CKD-induced IL-1β cleavage in microglia. (**a**) GEO Biological process (BP) analysis summarizing the DEGs in microglia of sham-operated or 5/6-nephrectomized

mice (CKD) identified by snRNA-seq. Highlighted (yellow) are the BP which are related to inflammation or immune response.

(**b**) Heatmap summarizing the DEGs in microglia of sham-operated or 5/6-nephrectomized mice (CKD) identified by snRNA-seq. Counts larger than the average are in yellow; counts lower than the average are in blue.

(**c**) Volcano plot depicting differentially expressed genes (DEGs) in microglia of sham-operated (sham) or 5/6-nephrectomized (CKD) mice. Red dots represent significant DEGs. The Y-axis denotes −log10 *p* values, while the X-axis shows log2FC values.

(**d**) IL-1β levels (ELISA) in the supernatant of caspase-8 knockout cells compared to control microglia treated with CKD or control plasma. The data shown represent the mean ± SEM.

(**e, f**) Example images of thallium-AMG (TlAMG, **e**) in neuronal cells cultured in conditioned medium (CM) obtained from microglia (MC) exposed to plasma obtained from patients with CKD (CKD Pl) or from healthy controls (C Pl). Casp1-knockout ($Casp1^{KO}$), $Casp8^{KO}$ or control (control plasmid, wild-type (WT)) microglia were used to generate the CM. Bar graph with dot plot (**f**) summarizing CTCD (corrected total cell density) of thallium-stained cells. Each dot represents number of positive cells in one field of view. Scale bar: 50 µm. *P* values were determined using one-way ANOVA with Dunnett's post hoc comparison.

Fig.4

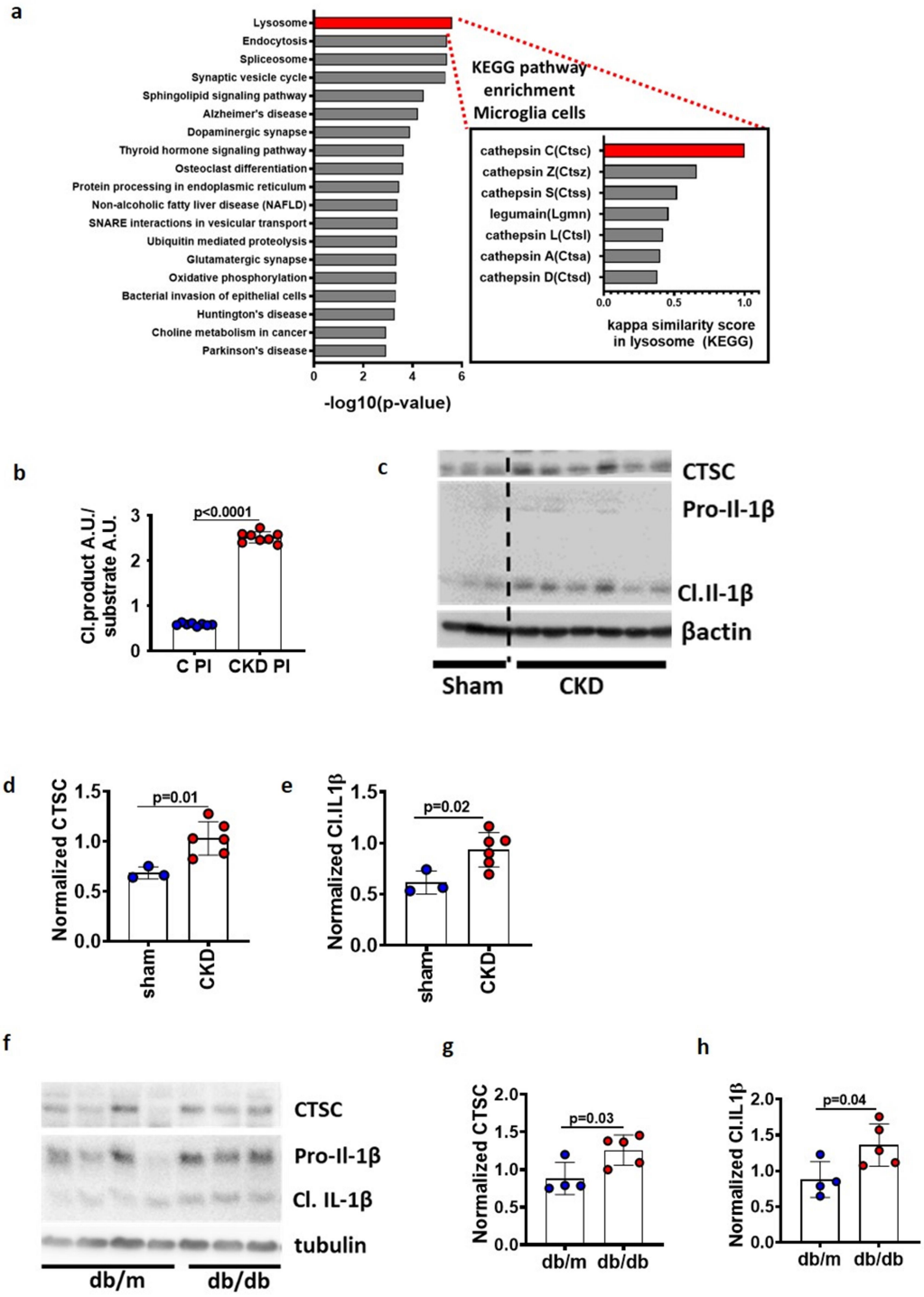

Figure 4

Lysosomal cathepsin C is activated in CKD in microglia. (**a**) Pathway analyses of the top enriched pathways (Kyoto Encyclopedia of Genes and Genomes (KEGG) analysis) for

differentially expressed genes (DEGs) in the microglial cluster of CKD murine brains compared to sham-operated murine brains (n=3 per condition). The log10 values of *p* values ($p < 0.05$) obtained after correcting for multiple testing (Benjamini–Hochberg correction) are shown.

(**b**) Cathepsin C (CTSC) activity, as determined by Gly-Phe beta-naphthylamide (GPN), in microglia exposed to C Pl or CKD Pl. Two-tailed Student's *t* test was used.

(**c-e**) Exemplary immunoblot images (c) and bar graph (d, e; mean ± SEM, each dot represents one biological sample) summarizing results of cathepsin C (CTSC, d), pro-Il-1β, cleaved Il-1β (e), and loading control β-actin expression in murine brain lysates of control (sham) or chronic kidney disease (CKD) ~~or diabetic (DM)~~ mice. *P* values: Two-tailed Student's *t* test was used.

(**f-h**) Exemplary immunoblot images (f) and bar graph (g, h; mean ± SEM, each dot represents one biological sample) summarizing results of cathepsin C (CTSC, g), pro-Il-1β, cleaved Il-1β (h), and loading control tubulin expression in murine brain lysates of control (db/m; ctrl) or diabetic (db/db; DM) mice. *P* values: Two-tailed Student's *t* test was used.

Fig. 5

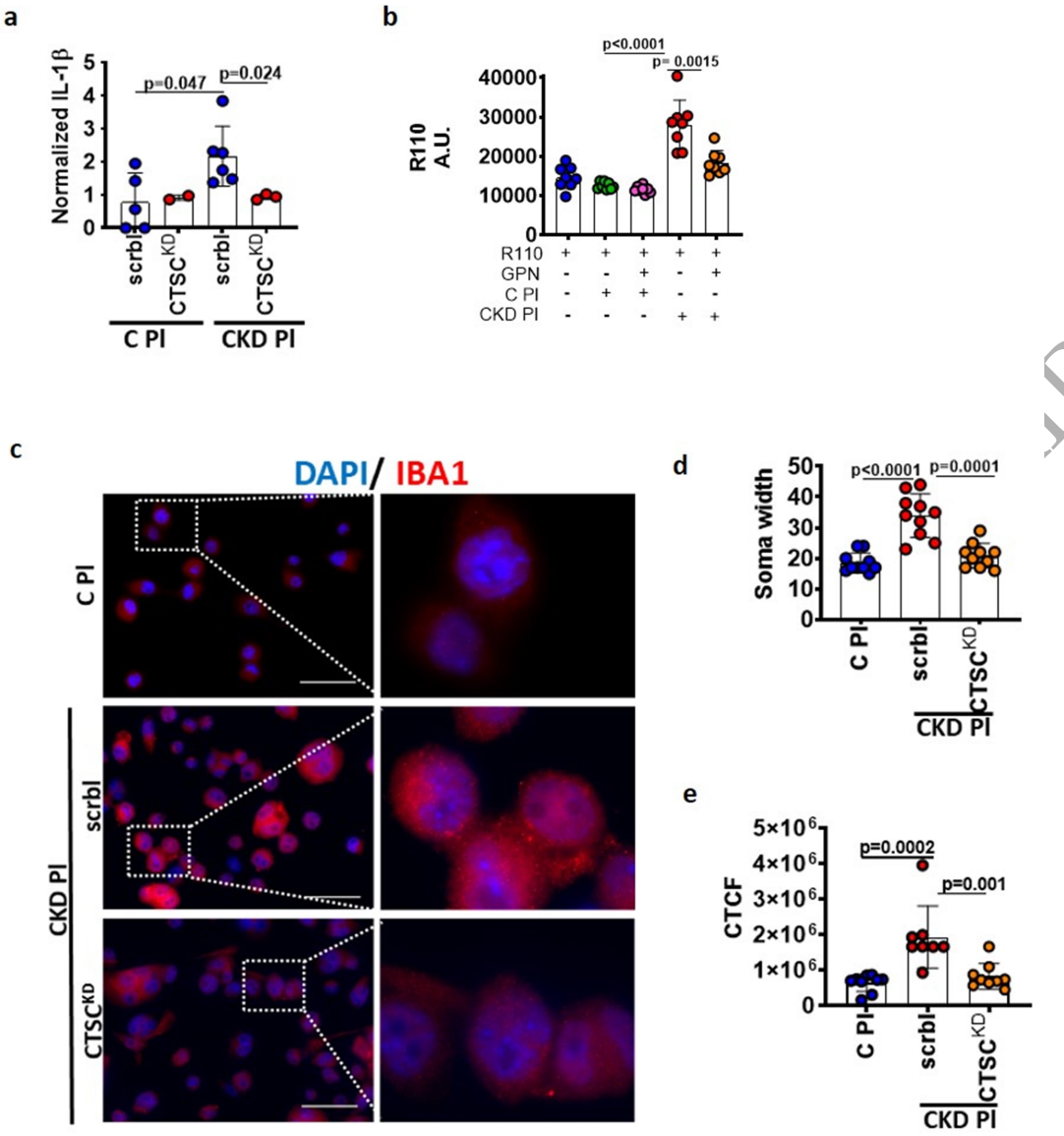

Figure 5

Lysosomal cathepsin C promotes microglia caspase-8 activation. (**a**) IL-1β levels (ELISA) in the supernatant of control microglia or CTSC-knockdown ($CTSC^{KD}$) microglia exposed to C PI or CKD PI; *p* values were determined using one-way ANOVA with Dunnett's post hoc comparison. Bar graph with dot plot; each dot represents one biological replicate. (**b**) Microglia loaded with fluorescent indicator-linked substrate for activated caspase-8 (R110) in C PI or CKD PI conditions; *p* values were determined using one-way ANOVA with Dunnett's post hoc comparison. Each dot represents the result of one biological replicate.

(**c**-**e**) Exemplary immunofluorescence images (**c**) of scrambled (Scrbl) control or cathepsin C knock down ($CTSC^{KD}$) microglia incubated with control plasma (C Pl) or chronic kidney disease plasma (CKD Pl) and stained for allograft inflammatory factor 1 (IBA1, red, a marker of microglia activation); DAPI nuclear counterstain (blue) and phalloidin (green). Scale bar: 50 µm. Bar graph (mean ± SEM, each dot represents the analysis of one field of view of 3 independent experiments) of soma width (d) and IBA1 quantified as corrected total cell fluorescence (CTCF, **e**). *P* values were determined using one-way ANOVA with Dunnett-post hoc comparison.